



**HAL**  
open science

## A Novel Method for Test and Calibration of Capacitive Accelerometers with a Fully Electrical Setup

Norbert Dumas, Florence Azaïs, Frédéric Mailly, Andrew Richardson, Pascal Nouet

► **To cite this version:**

Norbert Dumas, Florence Azaïs, Frédéric Mailly, Andrew Richardson, Pascal Nouet. A Novel Method for Test and Calibration of Capacitive Accelerometers with a Fully Electrical Setup. DDECS 2008 - 11th IEEE Workshop on Design and Diagnostics of Electronic Circuits and Systems, Apr 2008, Bratislava, Slovakia. 10.1109/DDECS.2008.4538807 . lirmm-00337873

**HAL Id: lirmm-00337873**

**<https://hal-lirmm.ccsd.cnrs.fr/lirmm-00337873v1>**

Submitted on 7 Sep 2022

**HAL** is a multi-disciplinary open access archive for the deposit and dissemination of scientific research documents, whether they are published or not. The documents may come from teaching and research institutions in France or abroad, or from public or private research centers.

L'archive ouverte pluridisciplinaire **HAL**, est destinée au dépôt et à la diffusion de documents scientifiques de niveau recherche, publiés ou non, émanant des établissements d'enseignement et de recherche français ou étrangers, des laboratoires publics ou privés.

# A novel method for test and calibration of capacitive accelerometers with a fully electrical setup

N. Dumas<sup>1</sup>, F. Azaïs<sup>1</sup>, F. Mailly<sup>1</sup>, A. Richardson<sup>2</sup>, P. Nouet<sup>1</sup>

<sup>1</sup> Université Montpellier 2 / CNRS

Laboratoire d'Informatique, de Robotique et de Microélectronique de Montpellier (LIRMM)  
161 Rue Ada, 34392 Montpellier Cedex 5, France

<sup>2</sup> Lancaster University, Centre for Microsystems, Lancaster, LA1 4YR, UK

*Abstract- Test and calibration cost is a bottleneck to reduce the overall production cost of MEMS sensors. One main reason is the cost of generating non electrical test stimuli. Hence, replacing the functional multi-domain test equipments with electrical ones arouses interest. The focus of this paper is on sensitivity testing and calibration through fully electrical measurements. A new method based on analytical expressions of the sensitivity with respect to both physical parameters of the structure and electrical test parameters is proposed. The accuracy of the method is evaluated by mean of a high level model including global and intra-die mismatch variations. It is shown that an accurate estimation of the sensitivity can be achieved using only electrical measurements and that the dispersions on the sensitivity can be divided by about 7 after the calibration procedure. These results are promising enough for high volume production of low-cost sensors.*

## I. INTRODUCTION

MEMS are multi-domain systems that benefit from the batch manufacturing capabilities of the semiconductor industry. Their implementation is increasing in applications requiring high volume and low cost. Their deployment for this kind of applications is expected to keep on growing, depending on the maturity of the manufacturing techniques. Therefore, there is a need to reduce the test cost which is an important part of the total manufacturing cost and to leverage the test techniques to high volume.

The classical test techniques for MEMS sensors are mainly functional. They basically consist in measuring directly all the specifications of the device. For example, to measure the specified sensitivity of an accelerometer, a calibrated acceleration is applied to the device through a shaker. However, the generation of calibrated non-electrical stimuli is generally more expensive than the generation of electrical stimuli and requires specific equipment for each type of sensor.

Recently, defect-oriented techniques based on electrical tests have been developed for surface micromachining [1] and bulk micromachining [2] technologies. Although they are proven efficient to detect specific defects, parametric variations are not considered and a final functional test remains often necessary to guarantee that all the products satisfy the specifications. Furthermore, the measurement of functional parameters is often necessary to calibrate the

device. Hence, there is a need to find new electrical tests to extract the specification parameters.

The fully electrical method proposed in [3], for capacitive MEMS accelerometers, shows a good potential for diagnosis and might be used for calibration. It is based on a finite element model that offers a good accuracy. Pull-in voltage and resonant frequency are measured to feed an algorithm that adjusts three parameters in order to match the model with the experiment. According to the authors, the model could be used for calibration once the adjustment procedure is done. However, the computation time needed by such technique is clearly prohibitive for production testing.

In this paper, we use an analytical method to extract the sensitivity of capacitive MEMS accelerometer from three parameters that can be measured electrically: the natural pulsation, the pull-in voltage and the electrostatic sensitivity. Once the sensitivity is estimated, it can be used for specification-based test or calibration. The paper is focused on the sensitivity because it is considered to be the most difficult parameter to estimate without a calibrated acceleration. For example, the offset can be directly electrically measured at the output of the sensor if the acceleration applied to the accelerometer is null. The method is clearly suitable for production in terms of computation time. The accuracy of the estimated sensitivity is evaluated using a high level model including mismatch.

The paper is organized as follows. First, the generic model of capacitive MEMS accelerometer is presented in section II together with the parametric fault model. The proposed method is then described in section III. Finally, evaluation results are presented in section IV.

## II. MODEL

### A. Accelerometer model

The device under test is a MEMS capacitive accelerometer with a differential structure formed by interdigitated fingers, as represented in Figure 1. This kind of structure is widely used and commercialized by some semiconductor manufacturers (e.g. Analog Devices). It is typically fabricated through surface micromachining and associated with CMOS electronic.

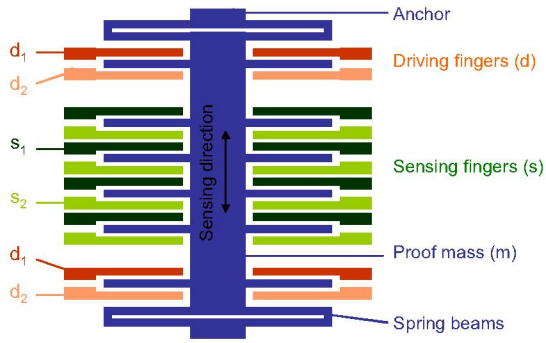


Figure 1. Schematic view of the accelerometer

The sensing electrodes measure the position of the proof mass. As shown in Figure 2, a high frequency carrier is applied on the two groups of sensing electrodes ( $s_1$  and  $s_2$ ). The signal picked up on the moving mass is read with a charge amplifier. At the output of the charge amplifier, the signal is a voltage centered on the carrier frequency whose amplitude is modulated by the position of the mass. It can be amplified again and demodulated to obtain an exploitable output signal  $V_{out}$ , which is a measure of the position and thus of the acceleration. The gain of the whole signal conditioning chain is designated as  $G$  in the following.

The previous mode of operation is the open-loop sensing mode. Apart from this mode, the driving fingers may be a mean to apply an electrostatic actuating force to the proof mass [3]. This is suitable to apply a test signal or to freeze the position of the mass whatever the acceleration is, in a closed-loop mode of operation. In this paper, we will use the driving fingers for test purpose only and we will consider that the accelerometer is used in open-loop architecture.

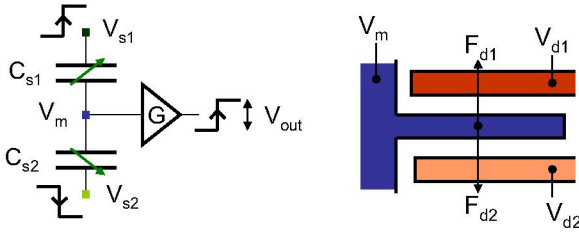


Figure 2. Capacitive reading (left) and actuating (right) principles

The accelerometer's proof mass, attached to the substrate with spring beams, is modeled with spring ( $K$ ), mass ( $M$ ), damping ( $D$ ) parameters and represented by a second order system, as depicted in Figure 3. The input is the sum of the forces induced by the acceleration of the device ( $A_m$ ) and the one induced by the actuating voltages. The output is the displacement of the mass with respect to its rest position. It is used to calculate the two output capacitances and the electrostatic actuating force.

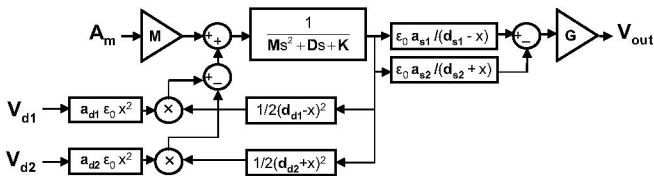


Figure 3. Block model of the accelerometer  
( $x$  represents the input of the considered block,  $s$  is the Laplace operator)

The description and nominal value of the model parameters are summarized in Table I. The values are inspired from the ADXL series accelerometer commercialized by Analogue Devices [4]. The resulting nominal natural frequency is 11.25 kHz. The structure has a low-damped resonant behavior with a quality factor equal to about 7. The capacitance variation is 0.347 fF for 1 g resulting in an overall sensitivity of 347 mV/g.

TABLE I  
NOMINAL MODEL PARAMETER VALUES

Symbol	Nominal parameters values		
	Description	Value	Unit
K	Spring constant	0.5	N.m <sup>-1</sup>
M	Proof mass	0.1	μg
D	Damping	1 10 <sup>-6</sup>	N.s.m <sup>-1</sup>
d	Distance between fingers. At nominal: $d_{s1}=d_{s2}=d_{d1}=d_{d2}=d$	1	μm
$a_s$	Sensing finger total area per group, facing the moving fingers. At nominal: $a_{s1}=a_{s2}=a_s$ .	10,000	μm <sup>2</sup>
$a_d$	Driving finger total area per group, facing the moving fingers. At nominal: $a_{d1}=a_{d2}=a_d$ .	3,000	μm <sup>2</sup>
G	Electrical gain = capacitance to voltage conversion coefficient × amplification gain	1	V/fF

### B. Parametric fault injection model

This paper is focused on parametric faults only. It is assumed that catastrophic faults such as break and stiction problems are easier to detect. Process scattering induces random variations of the properties and dimensions of the sensor. As a result, the spring, mass and damping parameters vary from one fabricated sensor to another and from one batch to another. Among a large quantity of fabricated sensors, each coefficient will be distributed around an expected value, i.e. typical mean value. In our model, we consider that each parameter has an independent normal distribution. In reality, correlations may exist between the  $K$ ,  $M$  and  $D$  coefficients. However, our distribution model can generate all the possible sets of parameters, including the ones that will be induced by the process scattering. Thus it is not a restrictive assumption to consider independent distributions, as the generated population will be larger than the real one but will include all possible devices.

The model also contains some dimension parameters: the areas of static fingers facing the moving ones and the distance between two consecutive fingers, for each group of fingers. The variations of these two parameters between two groups of fingers on the same sensor will be much lower than the variations between two sensors that may be fabricated on different wafers, different lots and different days. For instance, over- or under-etching faults will increase, respectively decrease, all the gap distances by approximately the same proportion. For this reason, we will consider two kinds of variations: global variations and intra-die mismatch. The global parameters are the average area ( $a$ ) and the average distance ( $d$ ) between the fingers, each one having an independent distribution. For each one of these global parameters, an independent mismatch parameter is

introduced to represent the variations between sensing / driving fingers and group 1 / group 2. Their expected value is 0 and their symbol is  $\alpha$  for the area and  $\delta$  for the distance. The eight dimension parameters of the model given in Figure 3 are finally defined by the following expressions:

$$\begin{aligned} a_{s1} &= a \times (1 - \alpha_{sd}/2) \times (1 - \alpha_{s12}/2) & d_{s1} &= g \times (1 - \delta_{sd}/2) \times (1 - \delta_{s12}/2) \\ a_{s2} &= a \times (1 - \alpha_{sd}/2) \times (1 + \alpha_{s12}/2) & d_{s2} &= g \times (1 - \delta_{sd}/2) \times (1 + \delta_{s12}/2) \\ a_{d1} &= (a \times k_d) \times (1 + \alpha_{sd}/2) \times (1 - \alpha_{d12}/2) & d_{d1} &= g \times (1 + \delta_{sd}/2) \times (1 - \delta_{d12}/2) \\ a_{d2} &= (a \times k_d) \times (1 + \alpha_{sd}/2) \times (1 + \alpha_{d12}/2) & d_{d2} &= g \times (1 + \delta_{sd}/2) \times (1 + \delta_{d12}/2) \end{aligned}$$

The generation of parametric faults on the distance between the sensing fingers is illustrated in Figure 4. The principle is the same for the area parameter. As the driving area is smaller than the sensing area, it is simply multiplied by a constant  $k_d$ , which is equal to 3/10 in the study. Hence, the global variations on the sensing and driving areas are identical relatively to the nominal value.

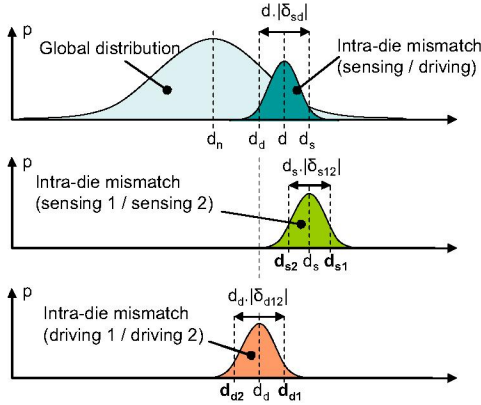


Figure 4. Distribution of the distance gap between fingers (determination of  $d_{s1}$ ,  $d_{s2}$ ,  $d_{d1}$  and  $d_{d2}$ )

As the electronic gain is taken into account in the model, global parametric variation will also be injected on  $G$ . In the following of the study, a normal distribution will be applied on each one of the global parameters:  $K$ ,  $M$ ,  $D$ ,  $d$ ,  $a$ ,  $G$ . If the process is stable, we consider that the expected value of these parameters will be their nominal value given in Table I. When intra-die mismatch is taken into account, a normal distribution is applied to each one of the mismatch parameters:  $\alpha_{sd}$ ,  $\alpha_{s12}$ ,  $\alpha_{d12}$ ,  $\delta_{sd}$ ,  $\delta_{s12}$ ,  $\delta_{d12}$ .

### III. TEST METHOD

The proposed test procedure assumes that the electronic stages have been tested and the overall gain has been characterised. Consequently,  $G$  will be a known parameter in the rest of the study. This may require additional design for test structures but this is not the focus of this paper. We also assume that the driving electrodes ( $V_{d1}$  and  $V_{d2}$ ) are externally accessible.

#### A. Electrical test parameters

##### 1) Natural pulsation: $\omega_0$

When operating at the natural pulsation, the output phase of the sensor is  $-90^\circ$  with respect to the sine input acceleration. One way to measure it electrically is to characterize the transfer function. Another way is to connect external components to build a PLL locking on  $-90^\circ$  phase shift; the natural frequency can then be deduced from the

VCO control voltage. Alternatively, other type of closed loop circuit can be used, as for example, the sensor put in an oscillator loop. The loop will oscillate at the resonant frequency. Here, the resonant frequency is very close to the natural frequency because the system is softly damped. The expression of the natural pulsation is given by:

$$\omega_0 = \sqrt{\frac{K}{M}} \quad (1)$$

##### 2) Static sensitivity to a small electrical signal: $S_v$

This parameter is derived from the average of two measurements: the sensitivity of the output  $V_{out}$  with respect to the square of a small signal applied to the input  $V_{d1}$  and the one with respect to  $V_{d2}$ . The electrical test setup is described in Figure 5.

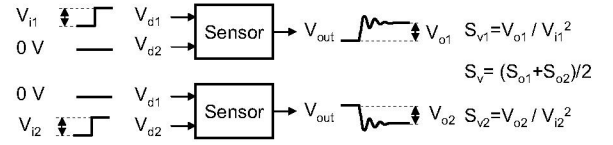


Figure 5. Electrical test setup for measuring  $S_v$

If no mismatch is considered, the small signal electrical sensitivities  $S_{v1}$ ,  $S_{v2}$  and the average  $S_v$  are equal. Under this condition  $S_v$  can be expressed by deriving the expression of  $V_{out}$  with respect to  $V_{d1}$  or  $V_{d2}$ . It results in:

$$S_v = \frac{G \cdot \epsilon_0^2 \cdot a^2 \cdot k_d}{K \cdot d^4} \quad (2)$$

##### 3) Pull-in voltage: $V_p$

The pull-in effect occurs when the spring force is not sufficient to compensate the electrostatic force. It can be observed by applying a voltage ramp on  $V_{d1}$  or  $V_{d2}$  (Figure 6). The ramp should be slow enough to maintain the sensor proof mass in a quasi-static state. The pull-in voltage is the input voltage at the time the absolute value of the output voltage changes suddenly and goes into saturation. If the saturation occurs before the pull-in voltage is reached, it can be measured by accessing an internal node in the signal conditioning chain where the electronic gain is lower. The electrical parameter  $V_p$  is the average of the pull-in voltages measured on both driving fingers.

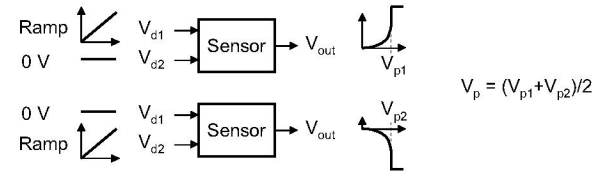


Figure 6. Electrical test setup for measuring  $V_p$

If the mismatch is neglected,  $V_{p1}$  and  $V_{p2}$  are the same and the expression of the pull-in parameter is given by [5]:

$$V_p = \sqrt{\frac{8 \cdot d^3 \cdot K}{27 \cdot \epsilon_0 \cdot (a \cdot k_d)}} \quad (3)$$

#### B. Expression of the sensitivity to the acceleration: $S$

Prior to express the sensitivity with respect to the electrical test parameters, we have to express it with respect to the model parameters. It can be expressed by deriving the

expression of the output with respect to the acceleration input. If intra-die mismatch is neglected, it results in:

$$S = \frac{2 \cdot G \cdot M \cdot \varepsilon_0 \cdot a}{K \cdot d^2} \quad (4)$$

The equations (1), (2), (3) and (4) form a system that can be solved if at least one of the following four model parameters is known: K, M, a, d. Assuming one out of the four parameters is known, the sensitivity can be expressed with respect to this parameter. It results in four expressions of the sensitivity:

$$S_d = \frac{1}{d} \cdot \frac{27 \cdot S_v \cdot V_p^2}{4 \cdot \omega_0^2} \quad (5)$$

$$S_a = \frac{1}{a} \cdot \frac{729 \cdot S_v^2 \cdot V_p^4}{32 \cdot G \cdot \varepsilon_0 \cdot \omega_0^2} \quad (6)$$

$$S_K = \sqrt{K} \cdot \frac{2 \cdot \sqrt{G \cdot S_v}}{\omega_0^2 \cdot \sqrt{k_d}} \quad (7)$$

$$S_M = \sqrt{M} \cdot \frac{2 \cdot \sqrt{G \cdot S_v}}{\omega_0 \cdot \sqrt{k_d}} \quad (8)$$

These expressions depend on the electrical test parameters defined in the previous section  $\omega_0$ ,  $S_v$ ,  $V_p$ , and on the model parameters K, M, a, d. For each fabricated sensor, the electrical test parameters can be measured. In contrast, the values of K, M, a, d are not precisely known for each fabricated sensor as they vary from one fabricated sensor to another. However, we can approximate them with a typical mean value. The error due to this approximation will be evaluated in the next section of the paper.

Finally, to obtain a single evaluation of the sensor sensitivity, we can make the average of the four previous expressions:

$$S_e = \frac{S_d + S_a + S_K + S_M}{4} \quad (9)$$

### C. Test & calibration procedure

This evaluation of the sensitivity ( $S_e$ ) from electrical parameters can be used for test and calibration. Manufacturers have to make sure that all the fabricated accelerometers are within the range given by the datasheet. For some low-cost applications, this tolerance range is in the order of +/-15%. It can be less than 1% for accuracy demanding applications. Usually, for capacitive MEMS accelerometers, the variation of the sensitivity of fabricated functional sensors is much larger than the tolerance range. A calibration of the sensitivity is therefore necessary to obtain satisfactory yield. It can be done by programming the gain of the signal conditioning chain through some fuses or an EEPROM. The calibration coefficient by which the gain has to be multiplied can be evaluated from the specified sensitivity  $S_{spec}$  and the evaluated sensitivity  $S_e$  by the ratio  $S_{spec} / S_e$ .

The evaluated sensitivity can also be used for test purpose. One can consider that a sensor should be rejected if its sensitivity is too far from the specified value. A big variation of sensitivity can reveal an intolerable defect. Furthermore, if the sensitivity is too low, the sensor resolution will be degraded. If the sensitivity is too high, the sensor dynamic range will be reduced. Therefore, a

tolerance range can be defined from the specified resolution and dynamic range. This is not the focus of the paper but the rejection of sensors can be included in the proposed procedure. The whole test and calibration procedure is summarized in Figure 7.

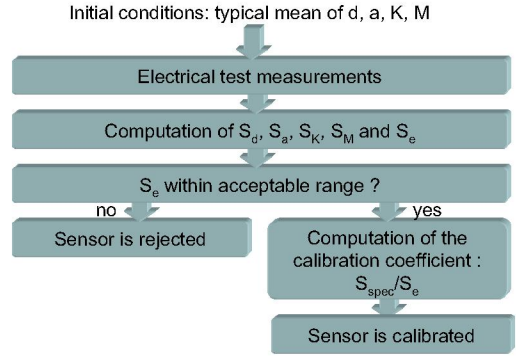


Figure 7. Flow chart of the test and calibration procedure

After the device is calibrated, its sensitivity has to be within the tolerance range. This will depend on the accuracy of the evaluated sensitivity.

## IV. EVALUATION OF THE METHOD

The evaluation consists in determining the accuracy of the evaluated sensitivity. For this purpose, the method is applied on a population of sensors, generated by Monte Carlo simulations with the parametric fault model described in section II. The method is first evaluated with ideal conditions, i.e. assuming there is no mismatch and the process is well-centered. We will then investigate the effect of mismatch and process drift on the accuracy of the evaluated sensitivity.

### A. No mismatch - Centered process

In this subsection, the mismatch parameters ( $\alpha_{sd}$ ,  $\alpha_{s12}$ ,  $\alpha_{d12}$ ,  $\delta_{sd}$ ,  $\delta_{s12}$ ,  $\delta_{d12}$ ) are set to zero. The expected values of the global parameters (K, M, D, d, a, G) are set to the nominal values (cf. Table I), which constitutes the initial conditions of the procedure. The standard deviation of the global parameters is set to 10% of the expected value. This results in a standard deviation of 30% on the real sensitivity distribution.

2000 Monte Carlo runs are simulated. For each simulation, the real sensitivity to the applied acceleration and the electrical test parameters are calculated. From the electrical test parameters and the initial conditions, the four sensitivities given by equations (5) to (8) are evaluated. Results are summarized in Figure 8, which presents the four evaluated sensitivities with respect to the real sensitivity. Each point corresponds to one sensor and the straight line corresponds to the ideal relation, i.e. the evaluated sensitivity is equal to the real sensitivity.

Two parameters can be calculated from the plot to assess how well the evaluated sensitivity fits the ideal line. The first one is the standard deviation of the evaluated sensitivity with respect to the real one:

$$\sigma_{sx} = std\left(\frac{S}{S_x}\right) \quad (10)$$

where  $\text{std}()$  is the standard deviation function. This figure of merit is equal to 0 if the ratio between the two sensitivities is constant. In other terms, it means that all the points of the graph are aligned on a line crossing the origin (0;0).

The second parameter is the difference between the mean of the sensitivity ratio and the ideal mean:

$$\mu_{S_x} = E\left(\frac{S}{S_x}\right) - 1 \quad (11)$$

where  $E()$  is the expected value function, i.e. mean function.

Ideally, this figure of merit is equal to 0. If both figures of merits are equal to 0, the evaluated sensitivity is exactly equal to the real one.

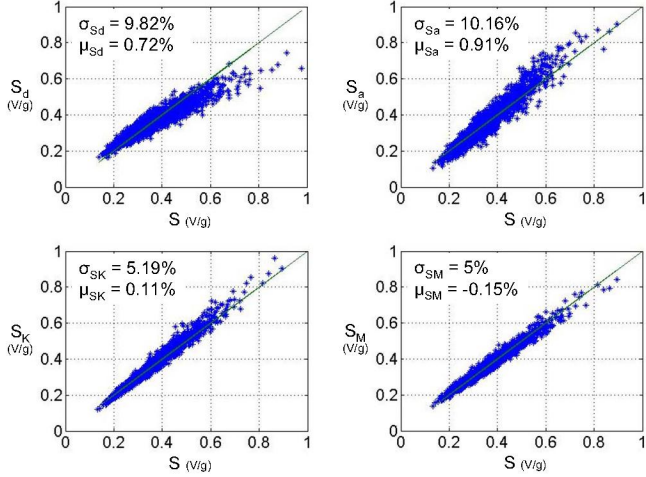


Figure 8. Plots of  $S_d$ ,  $S_a$ ,  $S_K$  and  $S_M$  with respect to the real sensitivity

Analyzing the results of Figure 8, we can observe that the relative mean figure  $\mu_{S_x}$  is very close to 0 for all of the four evaluations. It is to note that the same model is used for the simulations and the extraction of the four sensitivities; the parameter  $x$  is therefore the only unknown and source of error for the sensitivity  $S_x$ . Furthermore, as its value is set to the expected value in the process we are simulating, the error on the parameter  $x$  is null on average. Therefore, we simply observe that the error on the four evaluated sensitivities with respect to the real sensitivity is also null on average.

Apart from simulations, the standard deviation figures can also be deduced from uncertainty calculation. Taking into account that the error on the sensitivity  $\Delta S_x$  and the error on the initial condition parameters  $\Delta x$  are relatively small, the ratio of sensitivity can be expressed as follows:

$$\frac{S}{S_x} = \frac{S}{S + \Delta S_x} \approx 1 - \frac{\Delta S_x}{S} \approx 1 - \frac{\partial S_x}{\partial x}(x = x_n) \cdot \frac{\Delta x}{S} \quad (11)$$

with  $x = \{d, a, K, M\}$  and  $x_n$  being the nominal value of  $x$ .

For example, for  $S_K$  we have from equation (7):

$$S_K = S \cdot \frac{\sqrt{K_n}}{\sqrt{K}} \quad (12)$$

where  $K_n$  is the nominal spring constant value taken as an initial condition and  $K$  the actual value.

Applying equation (11) results in:

$$\sigma_{S_K} = \text{std}\left(\frac{S}{S_K}\right) \approx \text{std}\left(1 - \frac{1}{2} \frac{S \cdot K_n}{K_n^{3/2}} \frac{\Delta K}{S}\right) = \text{std}\left(\frac{\Delta K}{2 \cdot K_n}\right) \quad (13)$$

As the standard deviation on the global parameters has been set to 10% relatively to the nominal value, the standard deviation figure is 5% for  $S_K$ . By the same demonstration we found that  $\text{std}_{S_d}$  is 10%,  $\text{std}_{S_a}$  is 10% and  $\text{std}_{S_M}$  is 5%. These values are in agreement with the simulation results.

Finally, the evaluated sensor sensitivity ( $S_e$ ) can be computed as the average of the four sensitivities. This evaluated sensitivity is plotted in Figure 9 with respect to the real sensitivity. It can be seen that the standard deviation figure of merit is improved while the mean figure is still very good. This demonstrates the ability of the proposed method to accurately estimate the sensitivity of the sensor from electrical measurements, in case of a centered process with no mismatch.

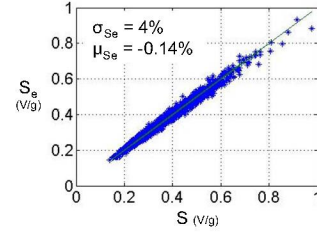


Figure 9. Plot of  $S_e$  with respect to the real sensitivity

To illustrate the calibration capability of the method, the sensitivity after calibration has been calculated for all the sensors by applying the calibration coefficient to the initial sensitivity  $S$ :

$$S_{cal} = S \times \frac{S_{spec}}{S_e} \quad (14)$$

The specified sensitivity is set to the nominal sensitivity value extracted from the model and the nominal model parameters values. It could be set to any value depending on the specification that is expected, without affecting the accuracy of the calibrated sensitivity. The distributions of the initial sensitivity  $S$  (before calibration) and the new sensitivity  $S_{cal}$  (after calibration) are presented in Figure 10. The relative difference of the expected value with respect to  $S_{spec}$  is directly given by the mean figure of  $S_e$ :

$$\frac{E(S_{cal}) - S_{spec}}{S_{spec}} = \mu_{S_e} \quad (15)$$

The standard deviation of  $S_{cal}$  relatively to the  $S_{spec}$  is directly given by the standard deviation of  $S_e$ :

$$\frac{\text{std}(S_{cal})}{S_{spec}} = \sigma_{S_e} \quad (16)$$

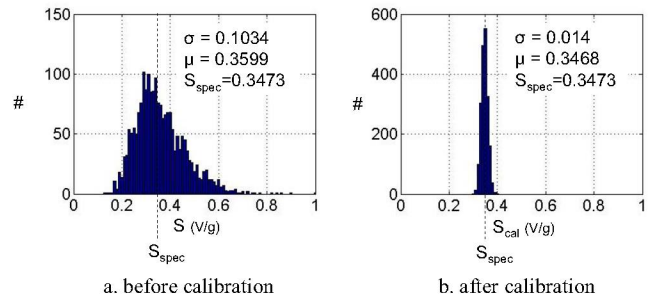


Figure 10. Distributions of  $S$  and  $S_{cal}$

We can observe in Figure 10 that the dispersion on the sensitivity is reduced by a factor 7.5. Furthermore, the sensor sensitivity is still centered on the specified value after

calibration; the centering on the nominal (and specified) value is even improved on the example of the Figure 10. The resulting maximal relative error is equal to 15.19%. This error is acceptable for some low-cost applications.

### B. Mismatch included - Centered process

In this subsection, the intra-die mismatches have been included in the simulation while we still assume that the process is centered on the nominal values of the model parameters. The standard deviation of the global parameters remains set to 10% and the standard deviation of the mismatch parameters is set to 2%. Such a mismatch results in a standard deviation of 7g for the equivalent input offset. Obviously, this value is unrealistic and shows how much the mismatch has been exaggerated.

As in the previous subsection, Monte-Carlo simulations have been conducted to generate a population of sensors. For each sensor of the population, the real sensitivity to the applied acceleration and the estimated sensitivities calculated from the electrical test parameters have been determined. Results are summarized in Table II in terms of figures of merit for the extracted sensitivities. It can be clearly seen that, despite the exaggerated mismatch taken into account, it has no significant impact on the accuracy of the evaluated sensitivity.

TABLE II  
EFFECT OF THE MISMATCH ON THE METHOD ACCURACY

Sensitivity	No mismatch		Mismatch	
	Mean % ( $\mu_{Sx}$ )	Standard deviation % ( $\sigma_{Sx}$ )	Mean % ( $\mu_{Sx}$ )	Standard deviation % ( $\sigma_{Sx}$ )
$S_d$	0.72	9.82	1.09	10.59
$S_a$	0.91	10.16	0.54	11.11
$S_K$	0.11	5.19	-0.13	5.49
$S_M$	-0.15	5	0.352	5.56
$S_e$	-0.14	4	-0.17	4

### C. No mismatch - Non-centered process

In this subsection, we consider that the process has drifted. Consequently, it is no longer centered on the typical mean values that have been characterized before. Although the mismatch has no significant impact, it has been removed to clearly see the effect of the process stability only. The expected value of d and a are changed by -20% and the one on K and M by +20%. According to equations (5) to (8) these variations are chosen in order to increase the values of the four sensitivities.

TABLE III  
EFFECT OF THE PROCESS CENTERING ON THE METHOD ACCURACY

Sensitivity	Centered		Not Centered (-20% on d and a +20% on K and M)	
	Mean % ( $\mu_{Sx}$ )	Standard deviation % ( $\sigma_{Sx}$ )	Mean % ( $\mu_{Sx}$ )	Standard deviation % ( $\sigma_{Sx}$ )
$S_d$	0.72	9.82	26.4	13.09
$S_a$	0.91	10.16	26.12	12.84
$S_K$	0.11	5.19	9.34	5.58
$S_M$	-0.15	5	9.42	5.5
$S_e$	-0.14	4	16.67	4.57

The figures of merit obtained under these conditions are summarized in Table III. It can be observed that the standard deviation is not strongly degraded. In contrast, the mean figure is significantly degraded.

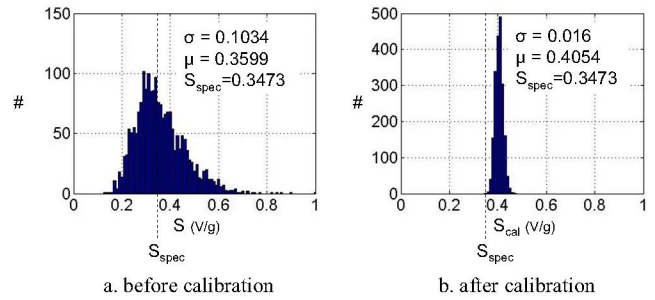


Figure 11. Distributions of the S and  $S_{cal}$  for a non-centered process

As we can see in Figure 11, the distribution of  $S_{cal}$  is no more centered on  $S_{spec}$ , introducing an error on the calibrated sensitivity. However, the maximal error between  $S_{spec}$  and  $S_{cal}$  is less than +40%, whereas the maximal error between the sensitivity S and  $S_{spec}$  was about +200%.

## IV. CONCLUSIONS & PERSPECTIVES

The proposed method shows potential for testing a large sensitivity variation due to process scatterings. It can be combined to existing fully electrical defect-oriented tests in order to guarantee good fault coverage.

It also offers a good potential for calibration of capacitive accelerometers in production. The dispersion on the sensitivity can be potentially improved by a factor 7 even if the device is subjected to strong intra-die mismatch variations. The accuracy could be suitable for test and production of low-cost products. Further evaluation will consist in using a more detailed model or sample devices to see the robustness of the method.

As the method assumes that the typical mean conditions of some model parameters are known to achieve a good accuracy, further improvements of the method concerns the improvement of the accuracy with respect to the process stability. The proposed method can also be improved if one parameter is subjected to less variation than the others or more information is known about it.

The method may have a potential for self-test and self-calibration as the all the measurements are electrical and may be done on-chip.

## REFERENCES

- [1] N. Deb and R.D. Blanton, "Multi-Model Built-In Self-Test for Symetric Microsystems", proceedings of VLSI Test Conference, pp. 139-147, 2004.
- [2] N. Dumas, F. Azaïs, L. Latorre and P. Nouet, "Electro-thermal stimuli for MEMS testing in FSBM technology", Journal of Electronic Testing: Theory and Applications, vol. 22, n° 2, pp. 189-198, April 2006.
- [3] L. Rocha, L. Mol, E. Cretu, R.F. Wolffenbuttel, J. M. da Silva, "Capacitive MEMS accelerometers testing mechanism for auto-calibration and long-term diagnostics", proceeding of IMSTW'07, Povoia de Varzim, Portugal, June 18-20 2007.
- [4] <http://www.analog.com/>
- [5] L. Rocha, E. Cretu, R. F. Wolffenbuttel, "Analysis and Analytical Modelling of Static Pull-In with Application to MEMS-based Voltage Reference and Process Monitoring", journal of Microelectromechanical Systems, vol. 13, pp. 342-254, 2004.